

Double-Crystalline Polyethylene-*b*-poly(ethylene oxide) with a Linear Polyethylene Block: Synthesis and Confined Crystallization in Self-Assembled Structure Formed from Aqueous Solution

Ting Li,[†] Wan Juan Wang,[†] Ran Liu,[†] Wei Hao Liang,[†] Guo Fang Zhao,[†] ZhiYun Li,[†] Qing Wu,^{†,‡} and Fang Ming Zhu^{*,†,‡}

Institute of Polymer Science, School of Chemistry and Chemical Engineering, Sun Yat-Sen University, Guangzhou, 510275, China, and Laboratory of Synthesis Design and Application of Polymer Materials, School of Chemistry and Chemical Engineering, Sun Yat-Sen University, Guangzhou, 510275, China

Received January 28, 2009; Revised Manuscript Received March 6, 2009

ABSTRACT: Narrowly distributed polyethylene-*b*-poly(ethylene oxide) diblock copolymers (PE-*b*-PEO) with a linear PE block were successfully synthesized by combination of click coupling reaction of azido-terminated polyethylene (PE-N₃) and alkynyl-terminated poly(ethylene oxide) (PEO-CONHCH₂C≡CH). PE-N₃ derived from tosylation and subsequent substitution by sodium azide of hydroxyl-terminated PE (PE-OH) which was prepared by means of chain shuttling ethylene polymerization with 2,6-bis[1-(2,6-dimethylphenyl)imino ethyl]pyridine iron (II) dichloride (complex 1)/methylaluminoxane (MAO)/diethyl zinc (ZnEt₂) and subsequent in situ oxidation with oxygen. PEO-CONHCH₂C≡CH was synthesized through esterification the hydroxyl end-group on hydroxyl-terminated PEO (PEO-OH) with phosgene and subsequent amidation by propargyl amine. The self-assembly of three double-crystalline PE-*b*-PEO samples with different block length in water were investigated by laser light scattering (LLS) and transmission electron microscopy (TEM). It was found that, in water, a solvent selectively good for the PEO block, PE-*b*-PEO chains with proper PE block length could form spherical multicores micelles with the insoluble and crystallized PE blocks as the multicores and the soluble and swollen PEO blocks as the shell. These multicores in one micelle could reaggregate to a single-core as temperature increased. Differential scanning calorimetry (DSC) experiments showed that the crystallization of both PE and PEO blocks was intensely confined by the previously self-assembled structure of PE-*b*-PEO in aqueous solution.

Introduction

The self-assembly of crystalline block copolymers have attracted a lot of research interests owing to the formation of unique aggregation morphology and the confined crystallization in the micro- and/or nanoscale self-assembled structure.^{1–25} Compared with the numerous research on self-assembly and crystallization of crystalline–amorphous diblock copolymers,^{1,3,8,10,13,15,16,20,23} the crystalline–crystalline (double-crystalline) diblock copolymers are much less reported.^{18,19,21,24,25} However, double-crystalline block copolymers have begun to be paid more attention, because more crystalline blocks can increase the complexity of the system, which may lead to unexpected novel properties such as banded spherulitic superstructures that progressively changed to spherical granular aggregates at lower supercoolings exhibited by double crystalline poly(*p*-dioxanone)-*b*-poly(*ε*-caprolactone) diblock copolymers.²⁵ Polyethylene-*b*-poly(ethylene oxide) (PE-*b*-PEO), a typical double-crystalline diblock copolymer, presents ordered self-assembled structures and confinement on crystallization in the melt.^{18,19,24} Sun et al.¹⁹ investigated the self-assembly and crystallization behavior of a well-defined low molecular weight PE-*b*-PEO diblock copolymers in the melt, indicating that extended-chain crystals were obtained for both blocks in a lamellar morphology. Additionally, the crystallization of the PEO blocks was confined between pre-existing PE crystalline lamellas. More recently, fractionated crystallization and fractionated melting of confined PEO microdomains in PE-*b*-PEO diblock copolymers have been observed by Müller et al.²⁴ Even

so, very little work on the influences of self-assembled structures formed from selective solvents on the confined crystallization of PE-*b*-PEO has been reported in the open literature.

In practice, the PE block in PE-*b*-PEO generally derives from poly(1,4-butadiene) prepared by living anionic polymerization and subsequent hydrogenation, which always contains 5–7% ethyl branches because of a certain fraction of 1,2-additions, exhibiting a nonuniform crystalline structure and a low crystallinity.^{2,4} To our knowledge, only Chung et al.²⁶ reported the synthesis of PE-*b*-PEO with linear PE block by the chain extension with living ring-opening polymerization of ethylene oxide based on a well-defined hydroxyl-terminated PE (PE-OH). In this case, borane-terminated PE was synthesized with metallocene catalyst in the presence of a dialkylborane (H-BR₂) chain transfer agent. The terminal borane group was then oxidated using NaOH/H₂O₂ to provide hydroxy-terminated PE-OH. However, their method afforded PE-OH with a broader molecular weight distribution $M_w/M_n \geq 2$. The introduction of chain shuttling ethylene polymerization^{27–29} seems to shed a light for the highly efficient preparation of end-functionalized PE with narrow molecular weight distribution. Growing polyethylene chains could shuttle between the chain growing center (CGC), a transition metal catalyst species, and such chain shuttling agents (CSA) as alkyl main-group metal or dialkyl-zinc, the latter serving as a reservoir of living chains, candidates for end-functionalized PE.^{27,29} Gibson et al.^{30–32} have reported that Zn-terminated PE could be prepared *via* chain shuttling ethylene polymerization performed with bis(imino)pyridine iron (II) complexes in combination with methylaluminoxane (MAO) and diethyl zinc (ZnEt₂). Click chemistry has been extensively used in polymer chemistry due to the high efficiency and technical simplicity of the reaction.^{33–43} Here, we report a new and suitable route for the synthesis of narrowly distributed PE-*b*-PEO with a linear PE block by click coupling

* Corresponding author. Telephone: (020) 84113250. Fax: (020) 84114033, E-mail: ceszfm@mail.sysu.edu.cn.

[†] Institute of Polymer Science, School of Chemistry and Chemical Engineering, Sun Yat-Sen University.

[‡] Laboratory of Synthesis Design and Application of Polymer Materials, School of Chemistry and Chemical Engineering, Sun Yat-Sen University.

reaction of alkynyl-terminated PEO (PEO-CONHCH₂C≡CH) with azido-terminated PE (PE-N₃) which rooted in chain shuttling ethylene polymerization with 2,6-bis[1-(2,6-dimethylphenyl)imino ethyl] pyridine iron (II) dichloride (complex **1**)/MAO/ZnEt₂. Furthermore, the self-assembly of the resultant PE-*b*-PEO in water was investigated by laser light scattering (LLS) and transmission electron microscopy (TEM), and then the confined crystallization of previously self-assembled PE-*b*-PEO samples in aqueous solution were investigated by differential scanning calorimetry (DSC).

Experimental Section

Materials. Polymerization-grade ethylene and extra-pure-grade nitrogen were dried by passing through a calcinated molecular sieves column. Toluene was refluxed over sodium/benzophenone and degassed with nitrogen. ZnEt₂ was purchased from Aldrich as a 1.0 mol/L hexane solution. Two PEO-OH were purchased from Sigma and was dried under vacuum at 60 °C for 24 h before use. Their molecular weight and molecular weight distribution were respectively determined by GPC to be $M_w = 1.6 \times 10^3$ ($M_w/M_n = 1.04$) and $M_w = 6.5 \times 10^3$ ($M_w/M_n = 1.15$). *p*-Toluenesulfonyl chloride (99%, TsCl), propargyl amine (99%), sodium azide (NaN₃, 99%), triphenylphosphine (PPh₃) and *n*-butyl lithium (2.5 mol/L solution in hexane, *n*-BuLi) were purchased from Acros and all were used as received. Phosgene toluene solution (20%) was purchased from Aldrich. CuBr (Acros, 98%) was purified according to the previous report.⁴⁴ All solvents and other reagents if not specified were purchased from Sinopharm Chemical Reagent Co., Ltd. S. Complex **1** was synthesized according to the literature procedure.^{30–32} Solid MAO was prepared by first the controlled reaction of trimethylaluminum (TMA) with H₂O from Al₂(SO₄)₃·18H₂O at a H₂O/TMA ratio of 1.3 dispersed in toluene for 12 h, then filtration, and finally evaporation under vacuum at 60 °C.

Synthesis of PE-OH. The chain shuttling ethylene polymerizations were carried out in a 300 mL steel reactor equipped with a mechanical stirrer at 25 °C. Complex **1** (3.0 mg, 5 μmol) and 50 mL of toluene was added to the reactor and then saturated with ethylene for 10 min, finally, MAO toluene solution (0.2 mol Al/L) and ZnEt₂ hexane solution (1.0 mol/L) were added to the reactor to start ethylene polymerization. The pressure of ethylene was maintained at 2.5 MPa. After 30 min, the polymerization mixture was heated to 100 °C, and dry oxygen was bubbled into the mixture for 2 h. Followed the oxidation reaction, the mixture was poured into HCl acidic methanol (500 mL) to precipitate the PE-OH. The white powder was filtered, washed with methanol, and then dried under vacuum at 60 °C. The ¹³C NMR measurement at 120 °C revealed that approximate 80% of the polyethylene chain has a hydroxyl end group.¹³C NMR (125 MHz, *o*-C₆D₄Cl₂, ppm): δ 64.3 (CH₂CH₂OH), δ 15.7 (CH₂CH₃).

Synthesis of PE-N₃. Anhydrous toluene (100 mL) was added into the dried PE-OH ([–OH] = 0.46 mmol) under nitrogen at 85 °C. The mixture was stirred for several hours until the PE-OH precursor dispersed into toluene, appearing homogeneous though with some extent opacity. When the PE-OH solution was cooled to 25 °C, 2.5 mol/L solution of *n*-butyl lithium in hexane (0.19 mL, 0.48 mmol *n*-BuLi) was added rapidly under stirring. After 30 min, anhydrous toluene solution of *p*-toluenesulfonyl chloride (0.19 g, 1.0 mmol, 10.0 mL) was added. The resultant mixture was stirred overnight at a refluxed temperature. The precipitate was filtered and the filtrate was evaporated under vacuum until it was dry. Through the purification of precipitating from *o*-dichlorobenzene to methanol three times, the precipitate was dried under vacuum at 50 °C for two days, the product of PE-OTs was obtained. Yield: ~96%. Sodium azide (0.15 g, 2.3 mmol) was added to a solution of PE-OTs (0.5 g, 0.23 mmol) in toluene/DMF (v/v = 3, 50 mL) with stirring at a refluxed temperature and allowed to react for 24 h. After the precipitation with methanol, the precipitate was washed with double distilled water and propanone respectively three times. Then the precipitate was dried under vacuum at 50 °C for two days, and 0.47 g PE-N₃ was obtained. Yield: 94.0%. ¹³C

NMR (125 MHz, *o*-C₆D₄Cl₂, ppm): δ 50.5 (CH₂CH₂N₃), δ 15.7 (CH₂CH₃).

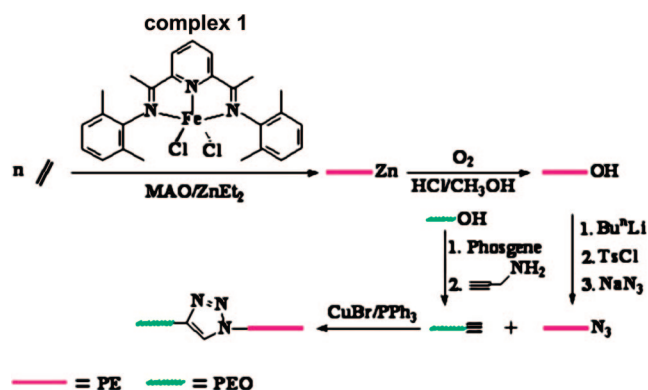
Synthesis of PEO-CONHCH₂C≡CH. PEO-OH ([–OH] = 11.5 mmol) was dissolved in dried toluene, refluxed, and dried under vacuum to remove water. Phosgene solution (15.0 mL, 20% in toluene) was then added into the dried PEO-OH with stirring. The reaction was allowed to proceed overnight in a fume hood. The excess phosgene was removed by evaporation under vacuum. 30.0 mL dichloromethane was used to dissolve the viscous residue. Propargyl amine (5.5 g, 0.1 mol) was then added into the solution. The reaction was allowed to proceed for 8 h at room temperature. The product was precipitated into Et₂O three times and dried under vacuum at 50 °C for two days, and PEO-C≡CH was obtained. Yield: ~80%. ¹H NMR (300 MHz, CD₃Cl, ppm): δ 2.25 (CH₂C≡CH), δ 3.81 (NCH₂C≡CH), δ 3.96 (OCOCH₂CH₂O), δ 4.05 (OCH₂CH₂O CO).

Synthesis of PE-*b*-PEO. Toluene/*o*-dichlorobenzene (v/v = 3), equimolar alkyl end group on PEO-CONHCH₂C≡CH ([–C≡CH] = 0.04 mmol) and azide end group on PE-N₃ ([–N₃] = 0.04 mmol) were introduced into a 100 mL Schlenk flask. The mixture was degassed with several cycles under vacuum and nitrogen. Before the click coupling reaction, the solution was stirred at 80 °C for 4 h to make the PE-N₃ dissolved as possible. The click coupling reaction was carried out when the catalysts CuBr (0.035 mmol) and triphenylphosphine (0.11 mmol) were added. After the coupling reaction took place for 24 h, the solvent in the reaction was removed by evaporation under vacuum, and the solid product was extracted by following Soxhlet extraction with THF for 8 h to remove the insoluble PE homopolymer. Then the soluble fraction of THF was condensed and poured into cold hexane in order to precipitate the resultant product. The obtained light yellow solid was dispersed into 3 mL of double distilled water by ultrasound, and the condensed dispersion was dialyzed against water at 25 °C for one week employing a dialysis bag ($M_p = 1 \times 10^4$) to exclude the unreacted PEO. In the end, the dispersion was washed with warm toluene four times. The organic phase was collected and concentrated under vacuum. By adding the organic phase into excess cold hexane, a precipitate was obtained. After this was dried under vacuum at 50 °C for 2 days, PE-*b*-PEO was obtained. The efficiency of click coupling reaction was ~85.5%. ¹H NMR (300 MHz, CD₃Cl, ppm): δ 2.04 (CH₂CH₂CH₂NNN), δ 4.26 (CH₂CH₂CH₂NNN), δ 7.62 (NNNCHCCH₂).

Measurements. Ambient temperature ¹H NMR (300 MHz) and ¹³C NMR (75 MHz) spectra were recorded in CDCl₃ on a Varian Unity Inova 300 spectrometer and high temperature ¹³C NMR (125 MHz) were performed on an INOVA 500 MHz spectrometer at 120 °C. Molecular weight and molecular weight distribution (M_w/M_n) were determined by gel permeation chromatography (GPC) against narrow molecular weight distribution polystyrene standards on a Waters 2414 refractive index detector at ambient temperature with THF as solvent or a Water 150C at 135 °C with 1,2,4-trichlorobenzene as solvent.

A commercial LLS spectrometer (Brookhaven BI-200SM) with a BI-9000AT digital correlator and a He-Ne laser at 532 nm was used. The samples were placed in an index-matching decalin bath with temperature control within ± 0.2 °C. Each solution was clarified by passing through a 0.45 μm PTFE filter to remove dust. A 3.0 mg/mL stock toluene solution of PE-*b*-PEO was prepared by the addition of 60.0 mg PE-*b*-PEO into 20.0 mL toluene, and the mixture was stirred at 25 °C for 24 h. A stock aqueous solution of PE-*b*-PEO with proper concentration was prepared by a slow addition of PE-*b*-PEO stock toluene solution to distilled water at 25 °C under stirring. After being stirred for 24 h at 25 °C, the solution mixture was set at 25 °C to remove the residual toluene floating on the water by volatilization. Both stock solutions were diluted to a proper concentration for the LLS measurement. The samples were equilibrated in the decalin bath at each temperature for 30 min before data collection. In static LLS, the average radius of gyration (R_g) and the averaged molar mass (M_w) of the micelles were determined, which led to the average aggregation number (N_{agg}) since the average molecular weight of individual

Scheme 1. Synthetic Route to PE-N₃, PEO-CONHCH₂C≡CH and PE-*b*-PEO



copolymer chains could be known by GPC. In dynamic LLS, the Laplace inversion of each measured intensity time-correlated function in a dilute solution can result in a characteristic line width distribution $G(\Gamma)$. For a purely diffusive relaxation, $G(\Gamma)$ can be converted to a hydrodynamic radius (R_h) distribution by using the Stokes-Einstein equation.

TEM observations were performed on a TEM (Philips TECNAI) with an accelerating voltage of 120 kV. To observe micelle morphologies under TEM yet retained the original morphological sizes and geometries as in aqueous solution, a drop from the previously prepared stock solution was deposited onto a carbon-coated copper grid. After a few minutes, the excess solution was blotted away with filter paper. The grids were dried at room temperature and atmospheric pressure for several hours before examination in the TEM.

DSC experiments were carried out on a Perkin-Elmer Pyris 1 instrument to study the melting behaviors of the PE-*b*-PEO. Samples of approximately 4 mg were encapsulated in aluminum pans. In this case, samples were obtained from toluene solution and aqueous solution at 25 and 60 °C respectively by vacuum evaporation at 25 °C and vacuum freezing and drying technology at -20 °C. The calibration was performed with indium and tin, and all tests were run employing ultra pure nitrogen as purge gas. DSC heating and cooling scans were performed at 5 °C/min over a temperature range of -50 to +150 °C.

Results and Discussion

Synthesis of PE-*b*-PEO. As shown in Scheme 1, chain shuttling ethylene polymerization was conducted with complex 1/MAO as catalyst and ZnEt₂ as CSA at 25 °C for 30 min. Zn-terminated PE afforded by transferring growing polyethylene chains from iron (II) species to zinc was oxidized by oxygen in situ at 100 °C and subsequently hydrolyzed to form PE-OH. At a ratio of Fe:Al:Zn = 1:100:500, a very narrow molecular weight distribution product was obtained (Figure 1, $M_w = 2.1 \times 10^3$, $M_w/M_n = 1.14$). And by ¹H NMR, the molecular weight of PE-OH was estimated about 2.0×10^3 . ¹³C NMR (Figure 2) spectrum revealed a saturated PE-OH based on the presence of the resonance peak at 64.3 ppm (CH₂CH₂OH)⁴² and no peaks attributable to chain end vinyl carbons between 100–150 ppm. The resonances of methine carbons between 38.0–40.0 ppm, which indicated the presence of a branched polyethylene, were not observed; therefore, the resultant PE-OH should have a linear structure. The efficiency of hydroxyl termination could be estimated to be near to 80% by comparison of the integrals of the resonance peak at 64.3 ppm and the peak at 15.7 ppm assigned to the chain end methyl carbons. PE-N₃ was then prepared through the two-step modification, the tosylation and the subsequent substitution by sodium azide, of PE-OH. In the ¹³C NMR spectrum (Figure 2), the signal of the methylene carbon adjacent to the azido group (CH₂CH₂N₃) was observed

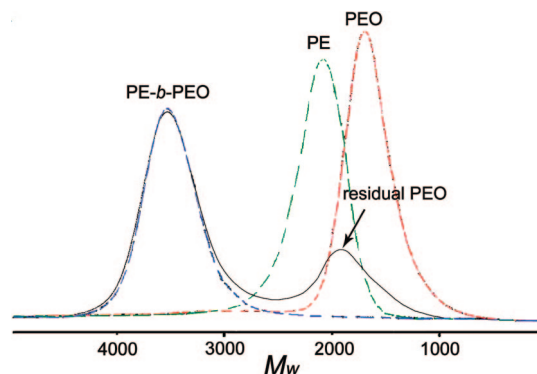


Figure 1. GPC profiles of PE and PEO precursors and their click coupling product, as well as the pure PE-*b*-PEO.

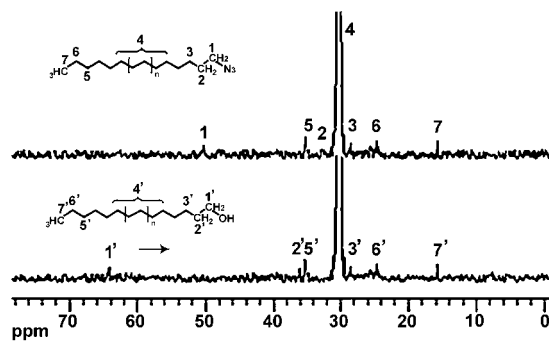


Figure 2. ¹³C NMR spectra of PE-OH and PE-N₃ obtained from chain shuttling ethylene polymerization and azidation of PE-OH ($M_w = 2.1 \times 10^3$).

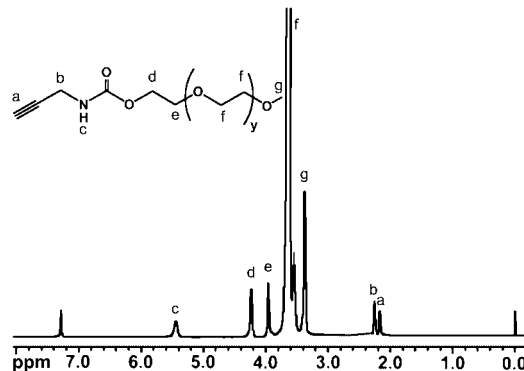


Figure 3. ¹H NMR spectrum of PEO-CONHCH₂C≡CH prepared by esterification with phosgene and subsequent amidation by propargyl amine of PEO-OH ($M_w = 1.6 \times 10^3$).

at 50.5 ppm. Moreover, no signals of the methylene carbon adjacent to the hydroxyl end-groups (CH₂CH₂OH δ 64.30 ppm)⁴⁵ and the methyl carbon (C₆H₄CH₃ δ 21.64 ppm)⁴⁴ in tosyl were detected. These results indicated that the conversion from PE-OH into PE-N₃ was almost 100%. Another PE-N₃ ($M_w = 1.0 \times 10^3$, $M_w/M_n = 1.08$) was synthesized at Fe:Al:Zn = 1:100:750. PEO-CONHCH₂C≡CH was synthesized *via* esterification the hydroxyl end-group on PEO-OH ($M_w = 1.6 \times 10^3$, $M_w/M_n = 1.04$) with phosgene and the subsequent amidation by propargyl amine.^{46–49} As presented in Figure 3, quantitative conversion to alkynyl end-groups was confirmed by ¹H NMR in terms of observing the appearance of the characteristic resonance peak at 2.25 ppm assigned to the hydrogen on alkynyl.⁵⁰ Another PEO-CONHCH₂C≡CH was also prepared with PEO-OH ($M_w = 6.5 \times 10^3$, $M_w/M_n = 1.15$).

A typical click coupling reaction of PE-N₃ ($M_w = 2.1 \times 10^3$) with PEO-CONHCH₂C≡CH ($M_w = 1.6 \times 10^3$) was

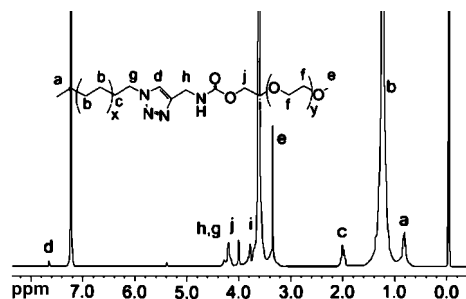


Figure 4. ^1H NMR spectrum of PE-*b*-PEO synthesized by click coupling reaction of PE- N_3 ($M_w = 2.1 \times 10^3$) with PEO- $\text{CONHCH}_2\text{C}\equiv\text{CH}$ ($M_w = 1.6 \times 10^3$).

performed with CuBr/triphenylphosphine (PPh_3) used as catalyst in toluene/*o*-dichlorobenzene ($v/v = 3$) at 80°C for 24 h. The coupling product was extracted by THF to remove PE (~ 20 wt %) which is insoluble in THF. As displayed in Figure 1, the GPC profiles shifted toward the high molecular weight region with a tail peak which could be attributed to the unreacted PEO precursor. Moreover, pure PE-*b*-PEO with 58 wt % PE was successfully obtained by dialysis against water with a dialysis bag ($M_p = 1 \times 10^4$) to remove PEO. The diblock copolymer formation efficiency was found to be 65.4% from the mass ratio of pure PE-*b*-PEO to click coupling product. The M_w (3.8×10^3) of the PE-*b*-PEO (Figure 1) with a narrow molecular weight distribution ($M_w/M_n = 1.21$) was the sum of M_w (2.1×10^3) of PE and M_w (1.6×10^3) of PEO. The ^1H NMR (Figure 4) characterization that the characteristic resonance peak at 7.62 ppm attributed to the proton of the newly formed five-membered triazole ring also confirmed the molecular structure of PE-*b*-PEO. The resonance assigned to methylene protons adjacent to the end functional group has moved from 3.27 ppm ($\text{CH}_2\text{CH}_2\text{N}_3$) to 4.26 ppm ($\text{CH}_2\text{CH}_2\text{CH}_2\text{NNN}$). These results demonstrated that the chain extension reaction in terms of click cyclization proceeded successfully, and a well-defined PE-*b*-PEO was prepared.

Self-Assembly of PE-*b*-PEO in Water. The self-assembly of PE-*b*-PEO with 58 wt % PE in water was carried out by a slow addition of a 3.0 mg/mL toluene solution of PE-*b*-PEO to water at 25°C under stirring. Note that PE-*b*-PEO diblock copolymers should self-assemble in toluene, a solvent selectively good for the PEO blocks.^{51,52} However, based on the investigation by dynamic LLS, the concentration of the stock toluene solution of the resultant PE-*b*-PEO ($C = 3.0$ mg/mL) is lower than the critical micelle concentration (CMC), at which PE-*b*-PEO individual chains could not aggregate. After the PE-*b*-PEO individual chains diffused into water phase, the residual toluene floated on water was then removed by volatilization at 25°C . In this case, the self-assembly of PE-*b*-PEO chains in aqueous solution was investigated by LLS and TEM. The hydrodynamic radius (R_h) distributions determined by dynamic LLS at 25°C and $C = 42$ mg/L in Figure 5 showed a clear self-assembly of PE-*b*-PEO because the $R_h \sim 55$ nm was much larger than that of individual chains. Note that only one peak located at ~ 55 nm was detected on the R_h distribution, indicating the aggregation of all PE-*b*-PEO chains. Moreover, the sizes of the micelles were nearly independent of the PE-*b*-PEO concentrations in the 5.0–40 mg/L range and the self-assembly temperatures in the 20– 60°C range (Figure 6), implying that the aggregation number (N_{agg}) of PE-*b*-PEO chains nearly remained unchanged in these certain concentration or temperature range. Therefore, the averaged molar mass (M_w) and R_g of the micelles could be provided by static LLS based on the angular and concentration dependence of the average excess scattering intensity.

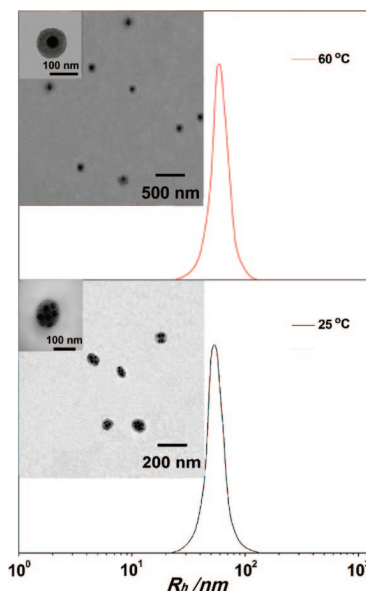


Figure 5. R_h distributions of the self-assembled PE-*b*-PEO with 58 wt % PE in water at 25 and 60°C . The inset shows the TEM microcopy of these micelles at 25 and 60°C .

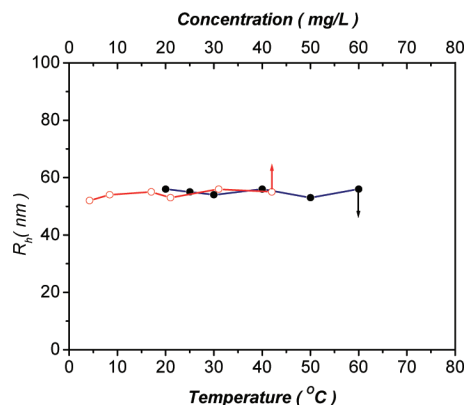


Figure 6. Changes of R_h as a function of temperature ($C = 42$ mg/L) or concentration (25°C) for PE-*b*-PEO (58 wt % PE) aqueous solution.

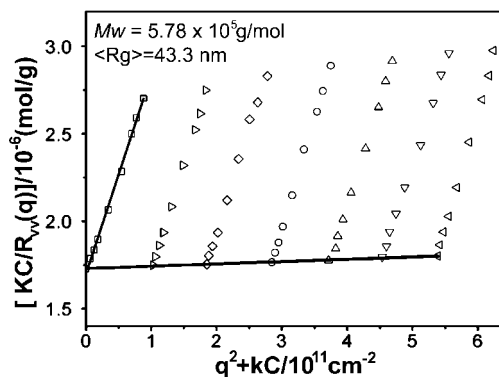


Figure 7. Zimm plot of PE-*b*-PEO chains with 58 wt % PE in aqueous solution at 25°C , where the concentration (C) is in the range 4.2–42 mg/L.

Figure 7 showed a typical Zimm-plot of PE-*b*-PEO in aqueous solution, where the correction of the concentration (C) of individual PE-*b*-PEO chains by subtracting the critical micelle concentration (cmc) was insignificant because cmc was rather low. On the basis of eq 1, the M_w and R_g of the micelles could

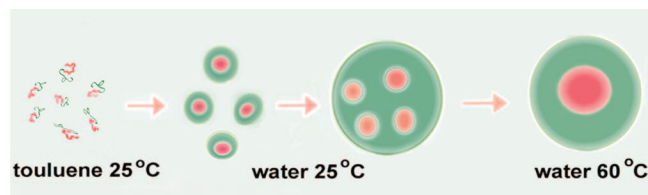


Figure 8. Schematic representation of multi self-assembly of PE-*b*-PEO diblock copolymer chains in aqueous solution.

be calculated to be 5.78×10^5 and 43.3 nm from the intercept of $[KC/R_{vv}(q)]_{q \rightarrow 0, C \rightarrow 0}$.

$$\frac{KC}{R_{vv}(q)} \approx \frac{1}{M_w} \left(1 + \frac{1}{3} \langle R_g \rangle^2 q^2 \right) + 2A_2C \quad (1)$$

where $K = 4\pi n^2 (dn/dC)^2 / (N_A \lambda_0^4)$ and $q = (4\pi n / \lambda_0) \sin(\theta/2)$ with N_A , dn/dC , n , and λ_0 being the Avogadro number, the specific refractive index increment, the solvent refractive index, and the wavelength of the light in a vacuum, respectively. A_2 is the second virial coefficient. From the M_w of these micelles and the GPC-determined molecular weight of individual PE-*b*-PEO chains ($M_w = 3.8 \times 10^3$), the N_{agg} of the PE-*b*-PEO chains inside each micelle was able to be calculated out to be about 152. On the other hand, the R_g/R_h ratio is calculated to be 0.787, indicating that the core of the micelles has a higher density, which agrees with the presumed core-shell structure.^{53,54}

As shown in Figure 5, the diameter of these self-assembled PE-*b*-PEO micelles, which retained the original morphological sizes and geometries as in the aqueous solution, explored by TEM here was very similar in size to that by dynamic LLS, which was about 105 nm for the spherical micelles with a broad distribution. Remarkably, multicores with a diameter of approximate 30 nm were observed in one micelle formed at 25 °C. The formation of these multicores micelles probably resulted from the aggregation of some small size micelles as shown in Figure 8. When the homogeneous toluene solution of PE-*b*-PEO was added into water, the individual PE-*b*-PEO chains could diffuse into water phase to form small size micelles. Consequently, small size micelles should reaggregate to form multicores micelles as soon as the PE-*b*-PEO concentration in water was increased as a result of minimizing the interfacial instabilities.⁵⁵ However, by increasing the temperature of the PE-*b*-PEO aqueous solution from 25 to 60 °C, only single-core micelles were observed and the diameter of the core grew to ~60 nm (Figure 6), but the sizes of the spherical micelles was nearly unchanged (~105 nm). The grown single-core is probably due to the reaggregation of these multicores in one micelle (Figure 8).

Effect of Block Length on the Properties of PE-*b*-PEO in Self-Assembled Structures. The block length of PE-*b*-PEO diblock copolymers had a serious influence on the self-assembly of PE-*b*-PEO chains in aqueous solution. Besides the PE-*b*-PEO with 58 wt % PE, two PE-*b*-PEO samples (sample 1, 39 wt % PE, $M_w = 2.6 \times 10^3$; sample 2, 14 wt % PE, $M_w = 7.4 \times 10^3$) have also been synthesized. The aqueous solutions of sample 1 (62.5 mg/L) and sample 2 (113.4 mg/L) were respectively prepared at 25 °C. As exhibited in Figure 9, multicores micelles could still be observed in the aqueous solution of sample 1 possessing the same PEO block length ($M_w = 1.6 \times 10^3$) as the PE-*b*-PEO with 58 wt % PE. However, the number of cores within one micelle reduced evidently to two or three. When the temperature of sample 1 aqueous solution was increased from 25 to 50 °C, and then isothermalized for 24 h, these small multicores in one micelle were aggregated into one big core while the size of the micelle was nearly unchanged ($R_h \sim 40$ nm), very similar to the PE-*b*-PEO sample

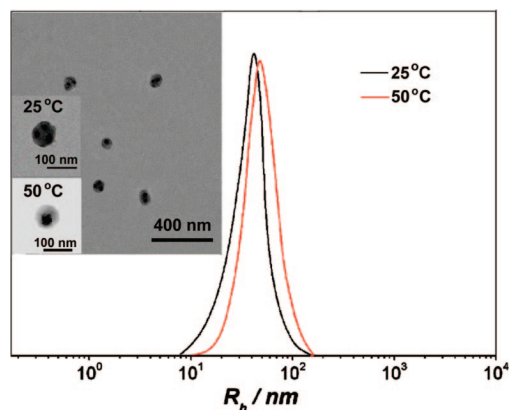


Figure 9. R_h distributions of the self-assembled PE-*b*-PEO with 39 wt % PE in water at 25 and 50 °C. The inset shows TEM microscopy of these micelles at 25 and 50 °C.

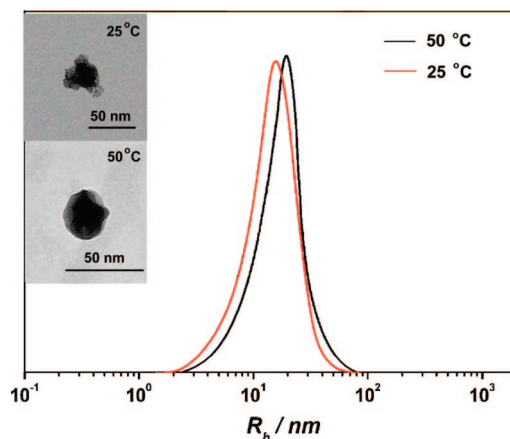


Figure 10. R_h distributions of the self-assembled PE-*b*-PEO with 14 wt % PE in water at 25 and 50 °C. The inset is TEM microscopy of these micelles at 25 and 50 °C.

with 58 wt % PE. For sample 2 with the same PE block length ($M_w = 1.0 \times 10^3$) as sample 1, no matter whether it was at 25 °C or at 50 °C, only one core could be observed in each micelles, and the R_h of micelles became smaller, ~20 nm (Figure 10). These results suggested that the much longer PEO blocks could afford enough interfacial areas to interact with water media *via* the hydrogen bond interaction.

Confined Crystallization of PE-*b*-PEO in Self-Assembled Structures. Figure 11 showed the DSC curves of three solid PE-*b*-PEO with 58 wt % PE samples prepared respectively from aqueous and toluene solution *via* vacuum freezing and drying technology and vacuum evaporation. The DSC curve of sample 3 obtained from toluene solution by vacuum evaporation at 25 °C displayed two melting temperatures (T_m) of PE blocks (88.7 °C) and PEO blocks (31.1 °C) which were lower temperature compared with corresponding homopolymers (122.3 and 36.4 °C). Note that there were several reports^{18,19,24} on the fractionated crystallization of PE-*b*-PEO when it was cooled from the melt. The crystallization of the PEO blocks was confined between pre-existing PE crystalline microdomains, while the crystallization of the PE blocks was almost not affected by PEO blocks, because PE has higher crystallization temperature than PEO. While the resultant PE-*b*-PEO chains might self-assemble to form micelles in the concentrated toluene solution as the solvent was removed by vacuum evaporation due to the insolubility of PE in toluene at 25 °C. Therefore, the T_m of PE blocks became so low about 88.7 °C in terms of the confined crystallization of PE blocks in the nanomicelles. The most

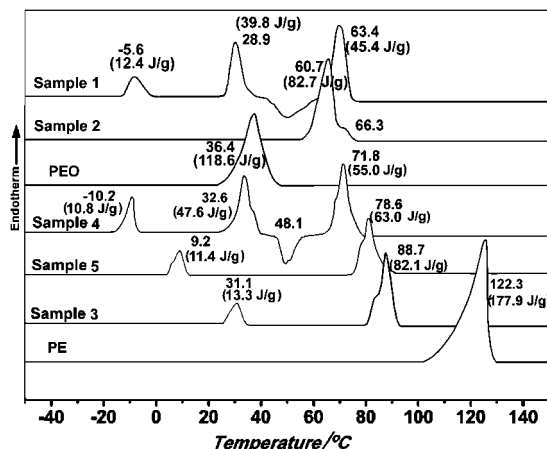


Figure 11. First DSC heating curves at 5 °C/min for PE ($M_w = 2.1 \times 10^3$) and PEO ($M_w = 1.6 \times 10^3$) homopolymers, PE-*b*-PEO with 58 wt % PE obtained respectively from toluene solution (sample 3), aqueous solution at 25 °C (sample 4) and 60 °C (sample 5), and sample 1 (39 wt % PE) and sample 2 (14 wt %) PE from aqueous solution at 25 °C.

interesting and novel behavior was observed for sample 4 obtained from the aqueous solution of self-assembled PE-*b*-PEO chains at 25 °C, which presented three melting endothermal peaks at 71.8, 32.6, and -10.2 °C and one cold crystallization exothermal peak at 48.1 °C. The endothermic enthalpy observed at 32.6 °C was detected to be 47.6 J/g (Figure 10). Hence this melting endotherm could only be attributed to PE blocks in that the melting enthalpy of PEO blocks of self-assembled PE-*b*-PEO should be obviously less than 48.9 J/g ($118.6 \text{ J/g} \times 0.42$). T_m of PE blocks at 32.6 °C was much lower because of the confined strongly crystallization of PE blocks in the very small nanodomains of multicores ($\sim 30 \text{ nm}$) existing in one micelle. Also, because the crystallization of PEO blocks was intensely confined by the multicores consisting of the crystallized PE blocks, its T_m was suppressed at such a low temperature of -10.2 °C. Note that the exothermal peak at 48.1 °C corresponding to the cold-crystallization of PE blocks clearly indicated the ordered reaggregation of the PE blocks within the multicores micelles and the formation of single-core micelles. Thus, it would be reasonable to believe that the higher T_m of PE blocks in the reforming single-core micelles could be observed at 71.8 °C. It is worth noting that the DSC curve of sample 5 obtained from the aqueous solution of self-assembled PE-*b*-PEO at 25 °C and then isothermalized at 60 °C overnight only presented two endothermal peaks of PE and PEO blocks at 78.6 and 9.2 °C, which was in agreement with the reaggregation of the multicores in one micelle with the increase of temperature observed by TEM. Moreover, the PE-*b*-PEO samples obtained not only from aqueous solution but also from toluene solution showed broad or bimodal melting endotherm of PE and PEO blocks. This result implied that the various confinement on crystallization of PE and PEO blocks by nanodomains with different sizes resulting from broader distribution of the self-assembled micelles (Figure 5).

Figure 11 showed the DSC curves of sample 1 and sample 2 obtained from aqueous solution *via* vacuum freezing and drying technology. As for sample 4 with 58 wt % PE, the DSC curve of sample 1 also displayed three melting endothermal peaks at 63.4, 28.9, and -5.6 °C and one cold crystallization exothermal peak at around 50.0 °C. Because the PEO block was longer than PE block in sample 1, compared with sample 4 the melting temperature (T_m) of PE blocks was lower, and the T_m of PEO blocks was increased. Comparatively, sample 2 only displayed two endotherms at 60.7 and 66.3 °C, which could be assigned

to PEO and PE blocks, basically in accordance with the TEM-observed microcopies.

In conclusion, PE-*b*-PEO diblock copolymer with a linear PE block was successfully synthesized by combination of chain shuttling ethylene polymerization and click coupling reaction. In water, a solvent selectively good for the PEO block, such as PE-*b*-PEO with proper PE block length at proper temperatures, could self-assemble to form spherical micelles possessing crystalline multicores, and these multicores could reaggregate as temperature increased. The crystallization of both PE and PEO blocks is intensely confined by the assembled structure of PE-*b*-PEO in aqueous solution.

Acknowledgment. The financial support of the National Natural Science Foundation of China (contract grant numbers 20574088, 20774109, and 20734004) and the Guangdong Natural Science Foundation (contract grant number 05003263) are gratefully acknowledged.

References and Notes

- Ryan, A. J.; Hamley, I. W.; Bras, W.; Bates, F. S. *Macromolecules* **1995**, *28*, 3860–3868.
- Hillmyer, M. A.; Frank, S. B. *Macromolecules* **1996**, *29*, 6994–7002.
- Quiram, D. J.; Register, R. A.; Marchand, G. R. *Macromolecules* **1997**, *30*, 4551–4558.
- Hillmyer, M. A.; Frank, S. B. *Macromol. Symp.* **1997**, *117*, 121–135.
- Manure, A. C.; Morales, R. A.; Sa'nchez, J. J.; Müller, A. J. *J. Appl. Polym. Sci.* **1997**, *66*, 2481–2493.
- Arnal, M. L.; Matos, M. E.; Morales, R. A.; Santana, O. O.; Müller, A. J. *Macromol. Chem. Phys.* **1998**, *199*, 2275–2288.
- Molinuevo, C. H.; Mendez, G. A.; Müller, A. J. *J. Appl. Polym. Sci.* **1998**, *70*, 1725–1735.
- Hamley, I. W.; Fairclough, J. P. A.; Bates, F. S.; Ryan, A. J. *Polymer* **1998**, *39*, 1429–1437.
- Arnal, M. L.; Müller, A. J. *Macromol. Chem. Phys.* **1999**, *200*, 2559–2576.
- Hamley, I. W. *Adv. Polym. Sci.* **1999**, *148*, 114–137.
- Manure, A.; Müller, A. J. *Macromol. Chem. Phys.* **2000**, *201*, 958–972.
- Arnal, M. L.; Müller, A. J.; Maiti, P.; Hikosaka, M. *Macromol. Chem. Phys.* **2000**, *201*, 2493–2504.
- Monkenbusch, M.; Schneiders, D.; Richter, D.; Willner, L.; Leube, W.; Fetters, L. J.; Huang, J. S.; Lin, M. *Physica B* **2000**, *276*–278, 941–943.
- Huang, W. H.; Luo, C. X.; Zhang, J. L.; Yu, K.; Han, Y. C. *Macromolecules* **2007**, *40*, 8022–8030.
- Chen, H. L.; Hsiao, S. C.; Lin, T. L.; Yamauchi, K.; Hasegawa, H.; Hashimoto, T. *Macromolecules* **2001**, *34*, 671–674.
- Loo, Y. L.; Register, R. A.; Ryan, A. J.; Dee, G. T. *Macromolecules* **2001**, *34*, 8968–8977.
- Yueh, L. L.; Richard, A. R.; Anthony, J. R. *Macromolecules* **2002**, *35*, 2365–2374.
- Sun, L.; Liu, Y. X.; Zhu, L.; Hsiao, B. S.; Avila-Orta, C. A. *Macromol. Rapid Commun.* **2004**, *25*, 853–857.
- Sun, L.; Liu, Y. X.; Zhu, L.; Hsiao, B. S.; Avila-Orta, C. A. *Polymer* **2004**, *45*, 8181–8193.
- Müller, A. J.; Balsamo, V.; Arnal, M. L. *Adv. Polym. Sci.* **2005**, *190*, 1–63.
- Hiroki, T.; Katsuhiko, F.; Takeshi, O.; Takayuki, O.; Masamitsu, M.; Katsuhiko, T.; Tomoo, S. *Polymer* **2006**, *47*, 8210–8218.
- Sinturel, C.; Vayer, M.; Erre, R.; Amennitsch, H. *Macromolecules* **2007**, *40*, 2532–2538.
- Chen, Y. F.; Zhang, F. B.; Xie, X. M.; Yuan, J. Y. *Polymer* **2007**, *48*, 2755–2761.
- Castillo, R. V.; Arnal, M. L.; Müller, A. J.; Hamley, I. W.; Castelletto, V.; Schmalz, H.; Abetz, V. *Macromolecules* **2008**, *41*, 879–889.
- Albuern, J.; Márquez, L.; Müller, A. J. *Macromolecules* **2003**, *36*, 1633–1644.
- Lu, Y. Y.; Hu, Y. L.; Wang, Z. M.; Manias, E.; Chung, T. C. *J. Polym. Sci., Part A: Polym. Chem.* **2002**, *40*, 3416–3425.
- Gibson, V. C. *Science* **2006**, *312*, 703–704.
- Arriola, D. J.; Carnahan, E. M.; Hustad, P. D.; Kuhlman, R. L.; Wenzel, T. T. *Science* **2006**, *312*, 714–719.
- Kempe, R. *Chem. Eur. J.* **2007**, *13*, 2764–2773.
- Britovsek, G. J. P.; Cohen, S. A.; Gibson, V. C.; Maddox, P. J.; Van Meurs, M. *Angew. Chem., Int. Ed.* **2002**, *41*, 489–491.
- Britovsek, G. J. P.; Cohen, S. A.; Gibson, V. C.; Meurs, M. V. *J. Am. Chem. Soc.* **2004**, *126*, 10701–10712.

- (32) Meurs, M. V.; Britovsek, G. J. P.; Gibson, V. C.; Cohen, S. A. *J. Am. Chem. Soc.* **2005**, *127*, 9913–9923.
- (33) Jiang, X. Z.; Zhang, J. A.; Zhou, Y. M.; Xu, J.; Liu, S. Y. *J. Polym. Sci., Part A: Polym. Chem.* **2008**, *46*, 860–871.
- (34) Fournier, D.; DuPrez, P. *Macromolecules* **2008**, *41*, 4622–4630.
- (35) Gondi, S. R.; Vogt, A. P.; Sumerlin, B. S. *Macromolecules* **2007**, *40*, 474–481.
- (36) Agut, W.; Taton, D.; Lecommandoux, S. B. *Macromolecules* **2007**, *40*, 5653–5661.
- (37) Ranjan, R.; Brittain, W. J. *Macromolecules* **2007**, *40*, 6217–6223.
- (38) Fournier, D.; Hoogenboom, R.; Schubert, U. S. *Chem. Soc. Rev.* **2007**, *36*, 1369–1380.
- (39) Hiki, S.; Kataoka, K. *Bioconjugate Chem.* **2007**, *18*, 2191–2196.
- (40) Gao, H. F.; Matyjaszewski, K. *J. Am. Chem. Soc.* **2007**, *129*, 6633–6639.
- (41) Liu, X. M.; Thakur, A.; Wang, D. *Biomacromolecules* **2007**, *8*, 2653–2658.
- (42) Gao, H. F.; Krzysztow Matyjaszewski, K. *Macromolecules* **2006**, *39*, 4960–4965.
- (43) Vogt, A. P.; Sumerlin, B. S. *Macromolecules* **2006**, *39*, 5286–5292.
- (44) Wang, J. S.; Matyjaszewski, K. *J. Am. Chem. Soc.* **1995**, *117*, 5614–5615.
- (45) Chul, J. H.; Mong, S. L.; Doo-Jin, B.; Sang, Y. K. *Macromolecules* **2002**, *35*, 8923–8925.
- (46) Zalipsky, S. *Bioconjugate Chem.* **1995**, *6*, 150–165.
- (47) Hiki, S.; Kataoka, K. *Bioconjugate Chem.* **2007**, *18*, 2191–2196.
- (48) Gao, H. F.; Matyjaszewski, K. *J. Am. Chem. Soc.* **2007**, *129*, 6633–6639.
- (49) Liu, X. M.; Thakur, A.; Wang, D. *Biomacromolecules* **2007**, *8*, 2653–2658.
- (50) Opsteen, J. A.; van Hest, J. C. M. *Chem. Commun.* **2005**, 57–59.
- (51) Lee, H. T.; Lee, D. S. *Macromol. Res.* **2002**, *10*, 359–364.
- (52) Tang, C. B.; Lennon, E. M.; Fredrickson, G. H.; Kramer, E. J. *Science* **2008**, 429–437.
- (53) Loscalzo, J.; Slayter, H.; Handin, R. I.; Farber, D. *Biophys. J.* **1986**, *49*, 49–50.
- (54) Wu, C.; Wang, X. H. *Phys. Rev. Lett.* **1998**, *80*, 4092–4094.
- (55) Zhu, J.; Hayward, R. C. *J. Am. Chem. Soc.* **2008**, *130*, 7496–7502.

MA900182S